CHEMICAL ENGINEERING TRANSACTIONS
VOL. 77, 2019
A publication of AIDIC
The Italian Association of Chemical Engineering
Online at www.cetjournal.it
Guest Editors: Genserik Reniers, Bruno Fabiano

ISBN 978-88-95608-74-7; **ISSN** 2283-9216
DOI: 10.3303/CET1977037

Masonry Failure and Debris Throw Characteristics under Dynamic Blast Loads

Johannes M. Schneider*, Malte von Ramin, Alexander Stottmeister, Alexander Stolz

Fraunhofer Institute for High-Speed Dynamics, Ernst-Mach-Institut, EMI, Am Klingelberg 1, 79588 Efringen-Kirchen, Germany
johannes.schneider@emi.fraunhofer.de

The hazard to persons and structures derived from secondary explosion effects, associated with blast loads on structural components resulting in e.g. debris throw, may exceed the hazard range from the blast wave itself. The debris throw hazard potential is related to the initial fragment throw parameters as launch velocities, angles and masses during the structural failure. These parameters strongly depend on the overpressure characteristics of the explosion, controlled by the explosive amount and category resulting in either detonations (typically high-order explosives, e.g. TNT or ANFO) or deflagrations (typically low-order explosives, as e.g. gas-air mixtures or propellants). Detonation shock fronts are typically characterized by very fast propagation velocities (supersonic), high peak overpressures and a small spatial extent. In contrast, the deflagration shock front propagates much slower (subsonic) and is characterized by lower peak overpressures but a larger spatial extent. Understanding the break-up process during the structural failure and the resultant initial fragment throw characteristics, related to the loading conditions (explosive amount and category), is thus essential to assess the hazard potential from explosions and provide the basis for proper consequence modelling in risk analyses. However, the data basis for hazard assessment and model development on debris throw from masonry structures is still very limited. This contribution describes recent shock-tube experiments with the goal to characterize the hazard from single span masonry walls subjected to dynamic blast loads with pressure-time characteristics of typical high-order explosions. Based on stereo high-speed video images and computer vision techniques, we analysed the masonry break-up process and derived debris fragment trajectories, velocities, launch angles and mass distributions. Based on the observed debris throw characteristics, approaches for hazard assessment of masonry failure are described in order to discuss the transferability of the results with respect to the different loading characteristics of low-order explosions and the structural component.

1. Introduction

Accidental and intentional conversion of explosives can lead to catastrophic damages to surrounding buildings and structures. The ensuing primary and secondary explosion effects, as fragment throw resulting from failing structural components, have the potential to cause severe injuries on exposed human bodies. In order to provide a robust hazard assessment related to debris throw originating from masonry structures, a deep understanding of the significant physical phenomena and their effects on the material and construction is essential. This includes an understanding of the masonry break-up and the resulting debris throw characteristics in terms of fragment launch masses, velocities and angles. However, to date, the data basis on masonry debris throw characteristics is very limited (Swisdak et al., 2007), challenging the hazard assessment from explosion driven masonry failures. Indeed, current practices and safety guidelines in the process industries commonly focus on the blast propagation and tend to neglect the debris hazard completely. Furthermore, aside from guidelines and standardization, the effects of deflagration type explosions on surrounding structures are still not fully understood. Within this study, a series of pneumatic shock tube tests on single-spanned masonry walls under varying loading conditions is presented. A high-speed stereo-camera

Paper Received: 20 February 2019; Revised: 11 May 2019; Accepted: 1 July 2019

Please cite this article as: Schneider J., von Ramin M., Stottmeister A., Stolz A., 2019, Masonry failure and debris throw characteristics under dynamic blast loads, Chemical Engineering Transactions, 77, 217-222 DOI:10.3303/CET1977037

video system and computer vision techniques were applied to determine mass distributions and debris flight trajectories. The data derived improve the assessment capabilities related to the hazard potential from interior explosions. Finally, the results are compared to explosions that are derived from deflagrations rather than detonations.

2. Methodology

2.1 Experimental setup

The experiments were conducted in a pneumatically driven shock tube at the Fraunhofer Institute for High-speed Dynamics (for more details see Schneider et al., 2019 and Stolz et al., 2016). Pressure gauges inside the shock tube measure the side-on and reflected pressure-time history of the simulated shock wave. Single spanned, single leaf masonry walls (1800 x 1500 mm) were fixed at the end of the shock tube, consisting of solid bricks with the dimensions of 240 x 115 x 52 mm (Figure 1). Three loading conditions were tested with reflected peak overpressures of 50, 100 and 150 kPa and maximum reflected impulses of ~ 400, 2000 and 3000 kPa ms, respectively, on average. Because the 50 kPa loading condition did not lead to masonry failure, the following analyses are related to 100 kPa peak overpressure and 150 kPa, respectively.

Figure 1: a): Shock tube at the Fraunhofer Institute for High-Speed Dynamics. b): Masonry wall specimen, at the end of the shock tube. Black markers on the brick faces are used for feature detection and automatic particle tracking.

2.2 High-speed stereo camera system

A major part of the analysis regarding mass distributions, launch angles and velocities is based on high-speed stereo video images. Two high-speed cameras (Photron Fastcam SA5 and SA1) were installed in approximately 6 m distances in front of the wall. The cameras recorded the experiments with a frame rate of 2000 fps. A stereo-calibration was performed in Matlab (Camera Calibration Toolbox for Matlab, http://www.vision.caltech.edu/bouguetj/calib_doc/) based on approximately 20 calibration images of checkerboard patterns in various orientations (Schneider et al., 2019). Uncertainties in the calculated 3D coordinates might derive from the accuracy of the camera calibration parameters and the accuracy of pixel coordinates of unique features in the left and right video images. For selected features with known dimensions, as the masonry framing or individual bricks, the absolute deviations of the calculated length scales compared to the true length scales ranged between 0 - 17 mm. Because the high frame rate of 2000 fps allows to smoothen trajectories and thus to average velocities over time, the accuracy of the system is sufficient to determine debris launch angles and velocities.

2.3 Mass distribution

Mass distributions of the masonry fragments were determined after the experiment by collecting, sorting and weighing the fragments, following the guidelines of TP21 (Swisdak et al., 2007). However, the mass distribution is considerably affected by shattering when the fragments hit the ground. Aiming to determine the kinetic energy from the particle mass and velocity, the mass distribution of the masonry debris (mortar and bricks) of each individual experiment was determined additionally based on visual analysis of the high-speed video images. For each individual experiment, fragment masses were estimated via their geometry, similar to the approach described in TP21 (Swisdak et al., 2007). Based on their geometry the fragments were assigned to size classes ranging from 1/8, 1/4 .. x/1 mortar fragment (where 1/1 mortar fragment size is defined as equal to the floor area of a brick) and 1/8, 1/4 .. x/1 bricks (Schneider et al., 2019). Using the fragment density these size classes where assigned to mass classes on a binary log-scale.

2.4 Fragment trajectories, launch velocities and angles

Fragment trajectories were determined based on a semi-automatic approach. In a first step, the black markers on the brick faces (Figure 1b) were roughly selected manually in the first left and right video images. The pixel coordinates of the exact marker centers were calculated based on the color differences between the marker and the surrounding brick color. In a second step, a simple automatic tracking algorithm determined the pixel coordinates of the markers over time (Figure 2, indicated as red dots), until the marker of an individual fragment got invisible (e.g. due to brick rotation or dust). In a third step, manually determined trajectories were added for mortar fragments and brick fragments for which no marker is visible. To do this, the fragment centroid (and the pixel coordinates, respectively) was determined based on the mean of the longest continuous fragment axis. Based on the 2D pixel coordinates on the left and right video images of individual fragments over time, the 3D coordinates were determined (Matlab, Stereo camera calibration toolbox for Matlab, more details see Schneider et al., 2019).

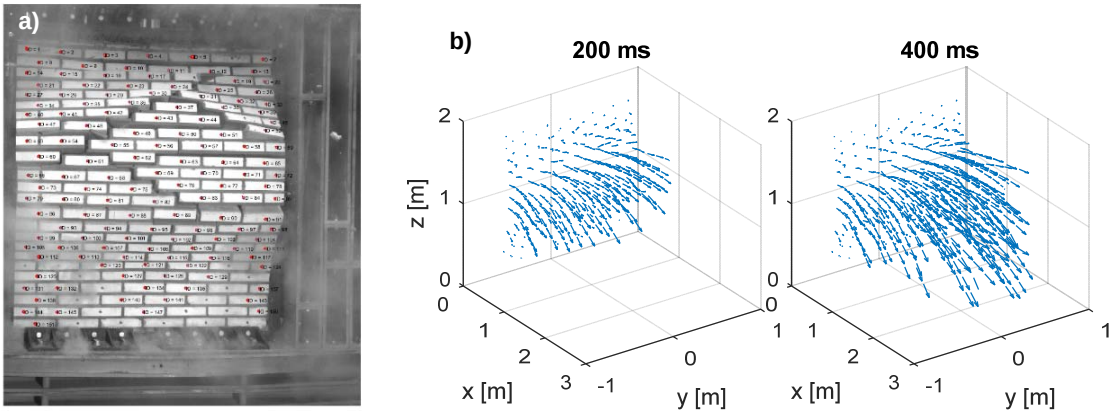

Figure 2: a): Masonry break-up after loading recorded from the left high-speed video camera. Red dots correspond to brick markers (black dots) that are used for feature detection and automatic fragment tracking. b): 3D trajectories, 200 and 400 ms after initiation (Schneider et al., 2019).

3. Results

3.1 Debris launch velocities

Fragment velocities were determined based on the distance between two coordinates related to travel times of 1, 10 and 20 milliseconds, whereas the 20 ms period was used in the further analysis as it smoothens out small-scale velocity variations, but shows well the overall velocity pattern (Schneider et al., 2019). In Figure 3a velocity profiles of all fragments and the median velocity of an individual experiment are shown related to the reflected pressure profile. Velocity values were binned in boxplots, including 25-75% of the velocity distribution, and whiskers including 9%-91% of the distribution at discrete time steps. Clearly, the velocity increases with increasing overpressure, however most acceleration occurs during the second overpressure peak, after the masonry wall was broken up from the first pressure increase. The spread of the velocity distribution after around 0.2 seconds is slightly increased, mainly due to the reduced number of fragments that can be analyzed during the later phase of the experiment.
Binning all velocity values of all experiments under a distinct loading condition and for discrete time steps clearly shows that the velocities tend to be higher for higher loading conditions (Figure 3b). Indeed, the mean velocity of the 150 kPa experiments is only 0.5-1 m/s higher than the mean velocities of the 100 kPa experiments after the second acceleration phase. However, the velocity distribution of the 150 kPa experiments includes also considerably higher fragment velocities up to approximately 11-12 m/s. In contrast, the distribution of the 100 kPa experiments is skewed in the other direction, with only a few values ranging above the mean, and more values considerably below the mean.

3.2 Debris launch angles

From the horizontal and vertical velocity components (Schneider et al., 2019), horizontal and vertical directions of motions over time were determined. The distributions of the vertical launch angles follow roughly a normal distribution (Figure 4b). The 150 kPa distribution is characterized by more positive values, compared to the 100 kPa distribution.

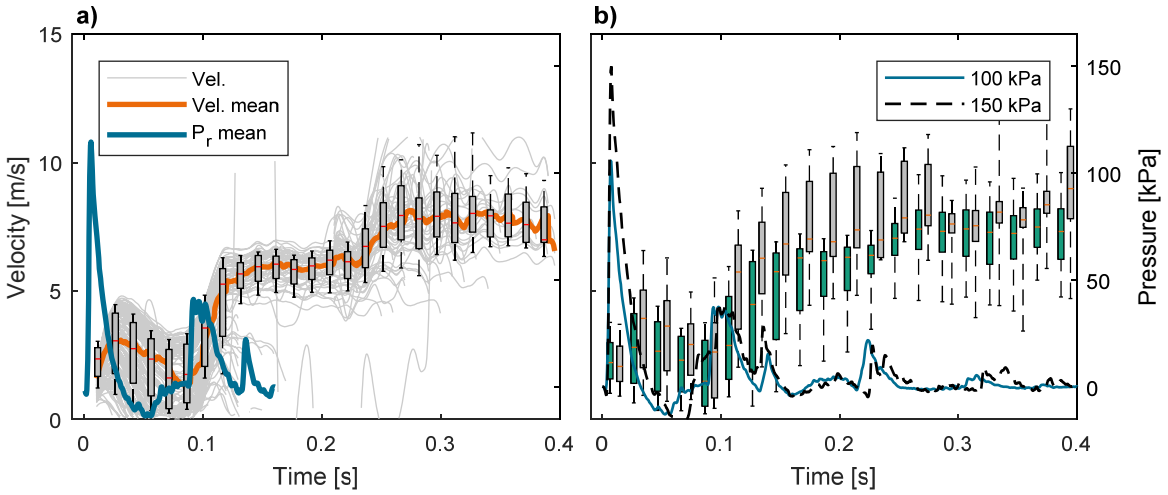

Figure 3: a) Individual (thin grey lines) and median (orange thick line) fragment velocities related to time for a specific experiment. The blue line represents the reflected overpressure. Boxes include 25% to 75% of the velocity distribution for the given time period, and whiskers include 9% to 91%. b) Velocity distributions for reflected peak overpressures with 100 kPa (green boxes) and 150 kPa (grey filled boxes) including all experiments (Schneider et al., 2019).

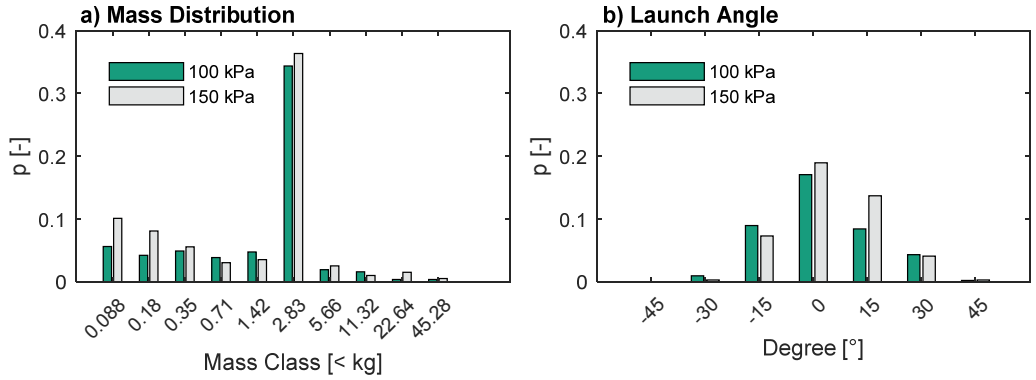

Figure 4: a) Mass distributions and b) vertical launch angle distributions related to the loading conditions. The number of fragments within each size is normalized by the total number of fragments. The 2.83 kg mass class, representing complete bricks, is the most dominant fraction.

3.3 Mass distribution

The distributions of debris masses were determined for the left and right video images separately, at least at two time-steps after initiation (200 and 400 ms). Within each mass class, the higher number of fragments from the left or right image, as well as from the different time steps were taken for further analysis. Doing so reduces the uncertainty having missed an individual fragment at a certain time step in an individual image. The 400 ms distributions are characterized by a slightly reduced number of total fragments compared to the 200 ms distributions, because some of the fragments moved out of the field of view. The derived mass distributions for each loading condition where averaged as presented in Figure 4. The mass class “2.83 kg” includes complete bricks and is obviously the most dominant size class.

4. Discussion

Debris throw from masonry failure adds a significant hazard potential to the blast wave hazard resulting from accidental or intentional driven explosions. However, to date the experimental data basis on masonry debris throw characteristics is very limited. This challenges the derivation of empirical relations (Ramin and Stolz, 2016) as well as the validation of numerical simulation methods for a proper hazard assessment of explosion driven masonry failures. The procedure, based on a high-speed stereo video camera system, allows (i) to

characterize mass distributions and (ii) to derive 3D trajectories in order to determine launch angles and velocities. In a subsequent step, the data compiled in this study will be used to assess the hazard originating from masonry failure under the given loading conditions. The fragment throw characteristics in terms of masses, initial velocities, and launch angles, provide the basis for empirical relations and the validation of deterministic model approaches. Hence, the established data contribute to an improved hazard management of explosives.

Despite the promising results presented in this study, several aspects and limitations need to be critically reviewed and discussed. A first limitation is the small range of overpressures investigated, ranging from 100-150 kPa peak overpressure. It remains unclear whether and how the results derived in this study can be extrapolated to higher loading conditions. The mass distributions of the two considered loading conditions are almost the same, with the most dominant size class corresponding to intact bricks. However, this does not allow the conclusion that the mass distribution is independent of the loading condition. In general, both sceneries could be possible: different loading conditions could result either in larger fragments (compounds of multiple fragments) or in smaller fragments by an increased amount of broken bricks. The velocity clearly increases with peak over-pressure, however it remains unclear to which extend the velocity would further increase in loading conditions higher than investigated in this study. With increasing loading, launch angles could be expected to move with less horizontal and vertical spread. For future investigations, it is suggested to use the results from this study to validate modelling tools that are able to simulate the break up process and the fragment throw of masonry walls related to the loading conditions. These validated models can then be used to predict debris throw characteristics also outside the pressure range investigated experimentally so far.

4.1 Comparison with weaker reaction types

The pressure profile of the presented experiments are related to a detonation shock front, which is typically characterized by very fast propagation velocities (supersonic), high peak overpressures and a small spatial extent. Aside from the experimental investigations on masonry structures provided in this study, in past years experiments were conducted at the Fraunhofer Institute for High-Speed Dynamics that provide a more general view on initial debris launch velocities (DLV) based on test slabs covering a rectangular steel box, in which a HE Pentolite charge was initiated (Dörr et al., 2002). The results of this study were compiled in the empirical DLV model (Eq. (1)),

$$DLV = C\sqrt{\frac{NEQ}{v^{2/3}\cdot\rho\cdot t}} \qquad \text{Eq. (1)}$$

where C= 525 m/s, NEQ is the equivalent TNT charge (net explosive quantity, kg), v= volume (m^3), p=slab density (kg/m^3) and t = slab thickness (m) (van der Voort and Weerheijm, 2013; Ramin and Stolz, 2016). However, in contrast to detonation shock fronts induced by high explosives, deflagration shock fronts, from e.g. accidental gas explosions in petrochemical surroundings, propagate much slower (subsonic) and are characterized by lower peak overpressures but cover a larger spatial extent (Ruming et al., 2011). The mechanical response in terms of fragment launch conditions of structural components under comparable energy densities, (lower peak overpressures but longer positive pressure duration), still has not been fully described.

Against this backdrop, the experimental research by Dörr et al. (2002) was recently repeated using gas-air mixtures instead of HE charges in order to determine initial launch velocities from deflagrations (Figure 5a). A stoichiometric 9.5 vol.% Methane-Air mixture inside a 0.07 m^3 vessel, corresponding to an energy density of a 40 g equivalent TNT charge, was ignited. The velocity of steel slabs (4 mm thickness) were determined using high-speed cameras (2000 fps). The pressure and impulse inside the vessel was calculated using the Apollo Blastsimulator (Klomfass et al., 2016, https://www.emi.fraunhofer.de/en/service-offers/software-solutions/apollo.html) for the methane-air mixture and for an equivalent 40 g TNT charge (Figure 5b). Whereas the peak overpressure is about an order of magnitude lower for the methane-air mixture compared to the TNT charge, the maximum impulses only differ roughly 20% between the two loading conditions. The preliminary analysis of the high-speed videos showed slab launch velocities of around 3 m/s. These velocities are more than an order of magnitude below the original DLV model, which predicts a velocity of about 60 m/s for a comparable loading density, despite the fact that the maximum impulses between the loading conditions are more or less the same. This observation highlights the need for further investigations on the physical responses of structural components to the blast loads from deflagrations in comparison to the loads from detonations. To complement the current results, the experimental series has to be completed, especially by varying the loading densities and relating the launch velocity to the quasi-static pressure inside the vessel or the corresponding energy content. The original DLV model (Eq. (1)) could then be the starting point for further

analysis and development of an empirical equation describing the initial debris launch conditions due to conversion of low order explosives resulting in deflagrations rather than detonations.

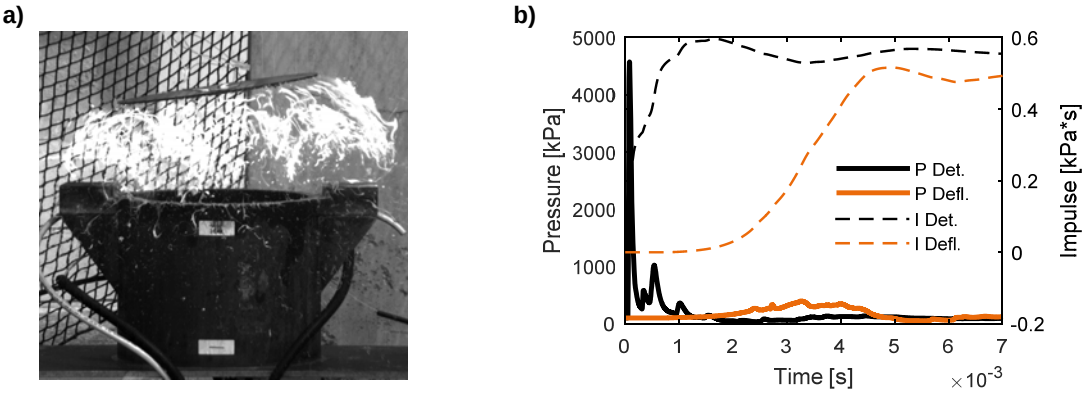

Figure 5: a) Deflagration slab-test using a stoichiometric Methane-Air mixture inside a 0.07 m^3 vessel (energy content comparable to an equivalent 40 g TNT charge). b) Simulated pressure and impulse profiles inside the vessel for the stoichiometric Methane-Air mixture (deflagration, abbreviated Defl.) and the comparable 40 g TNT charge (detonation, abbreviated Det.).

5. Conclusions

To date, the data availability on masonry debris throw characteristics is very limited, impeding the risk assessment and management of explosives in industrial surroundings. With this contribution, we established a method based on state-of-the-art computer vision techniques allowing determining 3D trajectories of masonry fragments. The data derived on the debris throw characteristics can be used for empirical hazard assessment due to explosion initiated masonry failures, as well as for the validation of deterministic simulation approaches. The methodology established in this study, combining shock tube experiments on masonry walls and stereo video analysis, can be used in principle to investigate in future experiments explosion effects not only related to detonations but also to deflagrations. This kind of conversion of explosives is especially of interest for industries handling with gases or where combustible dusts might be expected. For this purpose, the shock tube experiments can be adjusted to characterize the pressure-time profile of a typical deflagration, with lower peak overpressures but longer positive pressure durations accompanying a present experimental series initial debris launch velocities due to deflagrations.

References

Dörr, A., Michael, K., Gürke, G., 2002, Experimental Investigation of the Debris Launch Velocity from Internally Overloaded Concrete Structures, Final Report DLV 4-2002, Ernst-Mach-Institut, Fraunhofer Institute for High-Speed Dynamics (E 09/02).

Klomfass, A., Stolz, A., Hiermaier, S., 2016, Improved Explosion Consequence Analysis with Combined CFD and Damage Models. In: Chemical Engineering Transactions (48), 109–114, DOI: 10.3303/CET1648019.

Ramin, M. von, Stolz, A., 2016, Debris Throw Model for Accidental Explosions in a Complex Industrial Environment. In: Chemical Engineering Transactions (48), 85–90, DOI: 10.3303/CET1648015.

Ruming, Z., Baisheng, N., Xueqiu, H., Chao, W., Caihong, Z., Linchao, D., 2011, Different Gas Explosion Mechanisms and Explosion Suppression Techniques. In: Procedia Engineering 26, 1467–1472, DOI: 10.1016/j.proeng.2011.11.2326.

Schneider, J. M., Ramin, M. von, Stottmeister, A., Stolz, A., 2019, Characterization of debris throw from masonry wall sections subjected to blast. Under review, Engineering Structures.

Stolz, A., Millon, O., Klomfass, A., 2016, Analysis of the Resistance of Structural Components to Explosive Loading by Shock-Tube Tests and SDOF Models. In: Chemical Engineering Transactions (48), 151–156, DOI: 10.3303/CET1648026.

Swisdak, M. M., Tatom, J. W., Hoing, C. A., 2007, Procedures for the Collection, Analysis and Interpretation of Explosion-Produced Debris - Revision 1. Fort Belvoir, VA: Defense Technical Information Center.

van der Voort, M. M., Weerheijm, J., 2013, A statistical description of explosion produced debris dispersion. In: Int J Impact Eng 59, 29–37, DOI: 10.1016/j.ijimpeng.2013.03.002.